European Journal of Pharmaceutical Sciences 211 (2025) 107148

Contents lists available at ScienceDirect

European Journal of Pharmaceutical Sciences

journal homepage: www.elsevier.com/locate/ejps

# A peptide mimetic therapeutic strategy targeting dysfunction of the scaffold protein DISC-1 in psychiatric disorders

Abhishek Cukkemane [a,b,*], Andrew J. Dingley [a], Jeannine Mohrlüder [a], Beatrix Santiago-Schübel [a], Oliver H. Weiergräber [a,*], Dieter Willbold [a,b,*]

[a] Institute of Biological Information Processing, Structural Biochemistry (IBI-7), Forschungszentrum Jülich, Jülich, Germany
[b] Heinrich Heine University Düsseldorf, Institut für Physikalische Biologie, Düsseldorf, Germany

ARTICLE INFO

*Keywords:*
Schizophrenia
Disrupted in schizophrenia 1
Protein aggregation
Proteinopathy
Biophysical analysis
Drug development
Protein-protein interaction

ABSTRACT

Disrupted in schizophrenia 1 (DISC1) is a scaffold protein that regulates several physiological processes ranging from cellular division to neurodevelopment, and its dysfunction contributes to various neurological disorders including schizophrenia, bipolar and mood disorders, and autism. Thus, deciphering its native functions and pathophysiological roles is crucial. In this report, three disease-associated mutants of the C-region of DISC1, i.e., S713E, S704C, and L807-frameshift, were examined to further elucidate the role of DISC1 in cell division. We demonstrate that the mutations do not render the variants functionally inactive; instead, the interaction sites are presumably lost during the aggregation of the DISC1 C-region into amyloid-type fibrils. The minimal fibrillizing element in the C-region is the intrinsically disordered β-core (716–761) that houses a segment absent in the splice variant DISC1$^{\Delta 22aa}$, which cannot bind proteins of the mitotic spindle complex and thus hampers cellular proliferation. Based on these structure-function relationships, we present a rational drug development strategy using phage display technology and highlight the role of peptide mimetics in curtailing the agglomeration of fibrils.

## 1. Background

Schizophrenia, major depressive disorder (MDD), bipolar (BD) and autism spectrum disorders represent closely associated chronic mental illnesses (CMIs) that burden 3 %–5 % of the population (van Os and Kapur, 2009). Additionally, several aetiological factors, such as biological, environmental, social, and psychosocial conditions, are shared by these disorders but are still poorly understood. A critical biological risk factor that was discovered in a Scottish family with a diverse range of psychiatric disorders, including some affective CMIs, was the disrupted in schizophrenia 1 (DISC1) gene (Blackwood et al., 2001; Millar et al., 2000). Subsequently, studies of the cell biology (Brandon et al., 2004; Ishizuka et al., 2011; Kamiya et al., 2008), structural biology and biophysics of DISC1 (Cukkemane et al., 2021; Wang et al., 2019; Ye et al., 2017; Yerabham et al., 2018), as well as the characterization of mutant variants of the C-region (Ishizuka et al., 2011; Leliveld et al., 2008, 2009; Sachs et al., 2005) have added a wealth of information. Such mutations include the S704C, the S713E and L807-frameshift (L807-FS), which are of particular interest from a structural and functional perspective. For example, mutation of a single residue yielding S704C (Hashimoto et al., 2006; Leliveld et al., 2008, 2009; Narayanan et al., 2011) renders the protein highly insoluble. Consequently, in over 20 % of sixty cases from the biobank at the Stanley Medical Research Institute had the S704C mutant has been observed as aggregates in post-mortem brain tissue (Leliveld et al., 2008, 2009) from subjects suffering from schizophrenia, BD and MDD. The S713E mutant (Ishizuka et al., 2011) mimics a phosphorylation-related signaling cascade, responsible for the Bardet–Biedl syndrome, where neuronal progenitor cells cannot proliferate and migrate during corticogenesis. The L807-FS mutation piques our interest because this mutation causes severe schizophrenia and schizoaffective disorders and culminates in aggregated complexes (Sachs et al., 2005). Unlike the two Ser mutants, the L807 frameshift disrupts the normal reading frame downstream of L807 that comprise one of the binding sites for nuclear distribution element like 1 (NDEL1, formerly known as Nudel) (Brandon et al., 2004; Kamiya et al., 2006; Morris et al., 2003) in DISC1. The disruption of this DISC1–NDEL1 interaction hampers the formation of the mitotic spindle complex and associated cellular processes. These are a few examples

* Corresponding authors.
*E-mail addresses:* a.cukkemane@fz-juelich.de (A. Cukkemane), o.h.weiergraeber@fz-juelich.de (O.H. Weiergräber), dieter.willbold@hhu.de (D. Willbold).

https://doi.org/10.1016/j.ejps.2025.107148
Received 28 April 2025; Received in revised form 16 May 2025; Accepted 28 May 2025
Available online 29 May 2025

highlighting the pivotal role of the DISC1 C-region, which provides interaction sites for partners that regulate several key cellular processes, and is therefore of clinical relevance (Bradshaw and Korth, 2019; Hikida et al., 2012; Millar et al., 2003; Tropea et al., 2018; Yerabham et al., 2013).

DISC1 has evolved from being a gene that was initially linked to schizophrenia to a broader molecular candidate for therapeutic intervention in a range of CMIs and neurodevelopmental disorders. This conceptual expansion has led to the term "DISC1opathies", encompassing a spectrum of DISC1-driven protein conformational disorders rooted in disturbed proteostasis and non-genetic cellular stress (Korth, 2012). This includes a spectrum of DISC1-driven protein conformational disorders underlying disturbed proteostasis and non-genetic cellular stress (Bradshaw and Korth, 2019), which is similar in mechanism to classical neurodegenerative diseases (Cukkemane et al., 2021). These aggregates exhibit prion-like properties (Korth, 2012) and can recruit other proteins, such as dysbindin, enhancing their pathological impact. These findings are supported by postmortem analyses, in vitro assays, and animal models demonstrating that intracellular DISC1 misassembly is present in a significant subset of patients with CMI (Bradshaw and Korth, 2019). Furthermore, because DISC1 serves as a regulatory protein, several post-transcriptional modifications and the stability of its binding partners have also been considered as promising therapeutic targets (Hikida et al., 2012). Altogether, these insights highlight the relevance of DISC1 as a potential to bridge molecular pathology across psychiatric and neurodegenerative spectra.

Recent biophysical and structural biology characterization of the C-region revealed that the functional unit is a tetramer that binds NDEL1 and platelet activating factor acetylhydrolase 1b regulatory subunit 1 (PAFAH1B1, formerly LIS1) in a cooperative manner (Cukkemane et al., 2021). In contrast, aggregated DISC1 and its C-region (691–836) bind thioflavin T (ThT) (Cukkemane et al., 2021; Tanaka et al., 2017), indicating the formation of cross-β amyloidogenic fibrils. Under such conditions, the aggregated protein is most likely dysfunctional and a pseudo-repeat sequence, the β-core (716–761), was hypothesized to form the fibrillar axis (Cukkemane et al., 2021). This region houses part of the 22-residue stretch (748–769) that is absent in the DISC1$^{\Delta 22aa}$ splice variant (Kamiya et al., 2006; Taylor et al., 2003) and is critical for binding NDEL1 to promote neurite outgrowth. Here, we refer to this stretch as the Δ22 region.

Studying clinically identified mutants of the C-region of DISC1 should provide a wealth of information about DISC1 (dys)function. Moreover, it is critical to examine the significance of the β-core and the Δ22 region with respect to the common underlying theme, i.e., their interaction with nuclear distribution element 1 (NDE1, formerly known as NudE), NDEL1 and PAFAH1B1 in the mitotic spindle complex. Understanding the function in relation to protein structure should enable rational development of therapeutic agents targeting the DISC1 C-region. Therefore, to comprehend the effects of the DISC1 C-region mutants on the pathophysiology of schizophrenia and related CMIs, we employed a combination of biophysical and structural biology applications to shed light on DISC1 function.

We demonstrate the functional importance of the β-core for interaction with NDE1, NDEL1 and PAFAH1B1 and extend this analysis to the mutant proteins. In all cases, we observe nM affinity for the mutants to the above-mentioned protein partners. The findings strongly highlight the possibility that the loss of function involved in the pathophysiology of DISC1 and its mutants is not a primary consequence of mutations but rather results from pronounced aggregation. Next, using phage display technology, we identified several peptide hits targeting the wild-type (WT) monomeric and oligomeric versions of the DISC1 C-region. The top candidate peptides interacted with the C-region and mutant variants with high nM affinity. Their potential as drug candidates was studied using a combination of nuclear magnetic resonance (NMR) and dynamic light scattering (DLS) with the C-region, revealing that the peptides attenuate growth of DISC1 fibrils without requiring a specific binding site. The results provide insight into the poorly defined functional landscape of DISC1 and illustrate a strategy for developing drugs against DISC1 fibrillization.

## 2. Methodology

### 2.1. Protein expression and purification

The four DISC1 C-region constructs and the β-core (residue sequence in **Fig. S1)** in pESPRIT002 (Yumerefendi et al., 2010) were expressed separately as $His_6$-fusion constructs, as described previously (Cukkemane et al., 2021; Yerabham et al., 2018), by transforming *Escherichia coli* BL21 (DE3) pLysE T1R cells. Cultures were grown primarily in Luria-Bertani (LB) broth. Cells were cultivated in M9 minimal medium supplemented with $^{15}N$-$NH_4Cl$ for preparing NMR samples. Protein expression in minimal and rich media was induced by the addition of isopropyl-β-d-thiogalactopyranoside (IPTG) to a final concentration of 1 mM when cell cultures reached an optical density at 600 nm ($OD_{600}$) of ~0.6. Cells were then grown for 16 h at 18 °C. The cells were harvested and lysed in Tris-buffered saline (TBS; 10 mM Tris–HCl, 150 mM NaCl and Complete EDTA-free protease inhibitor cocktail (Roche), pH 7.4) using an ice-chilled microfluidizer M100P (Microfluidics MPT) at 15,000 psi. The insoluble fraction was removed by centrifugation at 50,000 × *g* for 25 min at 4 °C. The $His_6$-fusion construct was purified by loading the soluble fraction onto a column with $Co^{2+}$-charged NTA resin (Qiagen). The bound protein was eluted using TBS containing 500 mM imidazole. The $His_6$—C-region was further purified on a HiLoad 16/60 Superdex 200 size exclusion chromatography (SEC) column (GE Healthcare).

PAFAH1B1, NDE1 and NDEL1 were prepared using reported protocols (Cukkemane et al., 2021; Soares et al., 2012b; Yerabham et al., 2018). Briefly, PAFAH1B1 was expressed in *E. coli* BL21 C43 (DE3), whereas NDE1 and NDEL1 were expressed in *E. coli* BL21 (DE3) pLysE-T1R. The cells were cultivated at 37 °C until an $OD_{600}$ of 0.6, and expression was induced using 1 mM IPTG and cells grown for a further 16 h at 18 °C. As described above, the harvested cells were lysed and the soluble fraction loaded onto $Ni^{2+}$-NTA resin (Qiagen). After washing with TBS containing 20 mM imidazole, the target protein was eluted using TBS containing 500 mM imidazole and further purified on a HiLoad 16/60 Superdex 200 SEC column (GE Healthcare).

### 2.2. Circular dichroism (CD) spectroscopy

Far-UV CD spectra for the different C-region proteins were recorded using 20 μM samples in TBS on a Jasco J-1100 spectropolarimeter at 20 °C (0.2 cm path-length cuvette). The scan speed was 50 nm $min^{-1}$. Prior to the measurements, protein samples were centrifuged at 20,000 × *g* for 20 min at 4 °C to remove any potentially large aggregates and fibrils. The raw data obtained was normalized for the amino acid residues into mean residue ellipticity (MRE) to offer comparison between the different C-region variants and the β-core.

### 2.3. Dynamic light scattering (DLS)

Measurements of protein samples (10 μM) were performed using a SpectroSize 300 (XtalConcepts GmbH) instrument at 20 °C with a sample volume of 500 μL. Peptides were added to the protein sample at different ratios to study their effects on aggregation. Prior to measurements, all samples, without or with peptides, were centrifuged at 21,000 × *g* for 30 min at 4 °C. Diffusion coefficients were obtained from analysis of the decay of the scattered intensity autocorrelation function and were used to determine apparent hydrodynamic radii via the Stokes-Einstein equation, as implemented in the manufacturer's software (SpectroCrystal).

### 2.4. Phage display technique for identification of peptide hits

The phage display selection was performed as described previously (Santur et al., 2021) (**Fig. S2**) with a few modifications. Briefly, freshly prepared 100 μg/mL monomeric and 15 mg/mL a week-old oligomeric WT C-region DISC1 was used as targets for phage display selection, after immobilization on 3D—NHS matrix plates (PolyAn molecular surface engineering). During the selection rounds, the wells were blocked in alternate selections either with 22 mg/mL l-arginine or 15 mg/mL l-lysine. Multiple control selections were performed to ensure the quality of the selection starting from the library (TriCo16, Creative BioLabs). The different selection types were named "target selection" (TS), "direct control" (DC) and "empty selection" (ES). The ES was performed separately but analogously to the target selection without using the target protein. In the case of DC, the phages of the respective round of target selection were used as input but again no target protein was immobilized. Both control selections (ES and DC) were performed to enable reliable ranking of the resulting peptide sequences. Next-generation sequencing (NGS) of the phage DNA was performed at the Genomics & Transcriptomics Laboratory of the Heinrich-Heine-Universität Düsseldorf, Germany. For NGS, a sample from the library, and all TS, DS and ES inputs were prepared and sequenced.

The phage DNA sequences were processed and filtered using TSAT (target sequence analysis tool (Altendorf et al., 2024; Santur et al., 2021)). NGS data were filtered based on an overall increase in frequency of a sequence in the TS (library < TS1 < TS2 < TS3), enrichment because of the presence of the target in individual rounds (TS2 > DC2; TS3 > DC3) and lastly, enrichment with respect to a mock selection (TS1 > ES1; TS2 > ES2; TS3 > ES3). The resulting hits were ranked by enrichment score (TS3/library) and empty score (TS3/ES3). These filtered sequences were then used as input for HAMMOCK clustering (Krejci et al., 2016). From the list of peptides, we selected those with the highest enrichment scores from TS with the monomeric (Flm1) and oligomeric (Flo1) C-region proteins for further biophysical and structural characterization.

### 2.5. Biolayer interferometry (BLI)

Binding of physiological partners, i.e., PAFAH1B1, NDE1, and NDEL1 to the different DISC1 C-region constructs at protein concentration of 2 μM was studied using the Octet (ForteBio GmbH) instrument. Protein samples were dialyzed against phosphate buffered saline (PBS). The A2RG sensor chip (Sartorius GmbH) was activated with 1-ethyl-3-(3-dimethylaminopropyl) carbodiimide (EDC)/N-hydroxysuccinimide (NHS) (200 mM/50 mM) for coupling the ligand (C-region constructs). The peptides were diluted to 2 μM in 10 mM sodium acetate, pH 4.0, and immobilized to the sensor chip. The flow cell was deactivated with 100 mM ethanolamine-HCl, pH 8.5.

Binding of the peptides to the C-region constructs (WT, S713E, S704C, L807-FS, β-core) was investigated using a similar procedure. Peptides were dissolved in PBS prior to measurements, followed by coupling of the peptide-ligand to the A2RG sensor chip (Sartorius GmbH) using the activation and deactivation processes described above. The dissociation constant ($K_D$) was determined as the ratio of the off- and on-rate constants, using exponential dissociation and association fittings, respectively (OriginPro 2020, OriginLab, USA).

$$Association\ time{\rightarrow}y = y0 + A1 * \left(1 - \exp\left(-\frac{x}{t1}\right)\right) + A2 * \left(1 - \exp\left(-\frac{x}{t2}\right)\right)$$

$$Dissociation\ time{\rightarrow}y = y0 + A1 * exp\left(-\frac{x}{t1}\right) + A2 * \exp\left(-\frac{x}{t2}\right)$$

The rate constants ($k$) were derived by calculating the reciprocal of the average association/dissociation time ($t$), which was calculated as

$$\frac{1}{k} = t = \frac{A1 * t1 + A2 * t2}{A1 + A2}$$

The basic reaction describing the association/dissociation of the ligand-analyte interaction was represented as

$$[Ligand] + [Analyte] \rightleftharpoons [Ligand - Analyte]_{complex}$$

$$K_D = \frac{[Ligand - Analyte]_{complex}}{[Ligand][Analyte]} = \frac{k_{off}}{k_{on}}$$

The average dissociation constant and standard deviation of the ligand-analyte complex for DISC1-C-region constructs and β-core with the physiological partners is tabulated in Table S1 and the peptide-protein complex was measure once that is tabulated in Table S3. The inclusion criteria were sample dependent and greatly reflected on their stability. For instance, to determine the binding affinity of PAFAH1B 1 to the DISC1 C-region proteins, it was possible to have a sample count greater than 3, while for NDE1, due to its poor stability was limited to $n = 3$. The exact sample size for the measurements is described in Table S1 in supplementary section.

### 2.6. NMR experiments

Solution NMR experiments were performed at a $^{1}$H Larmor frequency of 750 MHz using a Bruker Avance III spectrometer equipped with a 5 mm cryogenic triple resonance probe. Measurements were performed at 25 °C. DISC1 C-region samples were prepared in PBS containing 10 % (v/v) $D_2O$ and 0.1 mM 2,2-dimethyl-2-silapentane-5-sulfonate (DSS). 2D $^{1}$H-$^{15}$N HSQC spectra were recorded in the absence and presence of peptide ligands. Proton chemical shifts were referenced to DSS and the $^{15}$N chemical shift was referenced indirectly (Wishart et al., 1995). Datasets were processed using Topsin 4.0.6 (Bruker Inc.) and analyzed using NMRFAM-Sparky (Lee et al., 2015).

### 2.7. Chemical cross-linking reaction and protein digestion

The oligomeric interface of the DISC1 C-region (WT and mutants) was examined by crosslinking experiments of C-region proteins (WT and mutants) coupled with mass spectrometry (MS) analysis. Preliminary tests were performed with DSBU (disuccinimidyl dibutyric urea), 1,1 carbonyldiimidazole (CDI) and disuccinimidyl sulfoxide (DSSO). We identified DSSO as suitable cross-linker. DISC1 C-region-protein (10 μg) samples were incubated for 1 h at 25 °C in the presence of excess of cross-linker (>1 mM) DSSO, which has a spacer arm length of 10.1 Å. The reactions were quenched by the addition of 500 mM Tris-Cl, pH 8.0 (final concentration). The samples were denatured in the presence of 1 % SDS and 10 mM DTT by heating to 95 °C for 10 min. After cooling the samples, cysteines were alkylated by incubation with 50 mM iodacetamide in darkness at 20 °C for 30 min. Next, 1 M DTT was added to a final concentration of 50 mM and the sample further incubated at 20 °C for 30 min to quench the reaction. For buffer exchange, single-pot solid phase (SP3) paramagnetic beads were used (Hughes et al., 2019). Proteins were bound to the beads by adding nine sample volumes acetonitrile (ACN, 90 % final concentration), washed with 90 % ACN, and released by reconstitution in digestion buffer containing 100 mM HEPES pH 7.5, 2.5 mM $CaCl_2$. Trypsin was added in a protein:protease ratio of 100:1 and incubated for 18 h at 37 °C. The samples were acidified to pH < 3.0 by adding 1 % formic acid and desalted by using self-packed double--layer C18-STAGE (STop And Go Extraction, 3 M USA)(Rappsilber et al., 2003) tips.

### 2.8. LC-MS/MS analysis

An estimated 1 μg of desalted peptides were loaded onto an Ultimate 3000 RSLC nano chromatography system (ThermoFischer) operating

with a two-column setup, a μPAC reversed-phase trap column (PharmaFluidics) and a 50 cm μPAC reversed-phase analytical column (PharmaFluidics), both equilibrated with 0.1 % formic acid in water, at a flow rate of 600 nL $min^{-1}$ and a column temperature of 40 °C. Bound peptides were recovered using a binary gradient from 2 % to 30 % of eluent (0.1 % formic acid in ACN), with 90 min effective separation time and a total runtime of 2 h per sample. Separated peptides were ionized using a CaptiveSpray nano-ESI source (Bruker) with the nitrogen gas saturated with ACN using a Nanobooster (Bruker) and introduced to an Impact II ultra-high resolution QqTOF MS (Bruker) as described in (Beck et al., 2015). Briefly, MS data was acquired with the Bruker HyStar Software (v5.1, Bruker) in line-mode with a mass range of 200−1750 m/z at an acquisition rate of 5 Hz. The 14 most intense ions were selected for fragmentation, with fragment spectra automatically acquired between 5 and 20 Hz. Selected precursors were excluded for the next 0.4 min unless the signal-to-noise ratio improved at least three-fold.

Cross-linked peptide fragments were subsequently identified using the software MaxLynx (Yilmaz et al., 2022) v.2.2.0.0 based on the amino acid sequences of the C-region proteins. The searches were performed using 10 ppm as the precursor, 20 ppm as the fragment ion precision and a false discovery rate of 1 %. Carbamidomethylation of cysteine side chains was assumed and variable degrees of N-terminus acetylation and methionine oxidation considered. Up to three missed cleavages of trypsin were allowed.

### 2.9. Structural models

The model of the DISC1 C-region protomer was obtained using AlphaFold2 (Jumper et al., 2021), and subjected to *in-silico* docking using CLUSPRO (Kozakov et al., 2017) in the multimer docking mode to generate models of the tetramer. The quality of the structural models was assessed using two sets of restraints, (i) the inter-subunit cross-link of K741-K741 from the MS data and (ii) the hydrodynamic radius ($R_H$) of the tetramer determined using DLS.

## 3. Results

### 3.1. DISC1 C-region mutants bind to their physiological partners

PAFAH1B1 and NDEL1 were previously shown by surface-plasmon resonance (SPR) to bind the native DISC1 C-region with nanomolar affinity (Cukkemane et al., 2021). However, the mutant proteins tended to aggregate readily and block the valves and capillaries of the SPR chip. NDEL1 and PAFAH1B1 were also susceptible to rapid precipitation in solution (Cukkemane et al., 2021; Soares et al., 2012a). These issues prohibited the use of SPR and thus the binding of the C-region variants with these physiological partners were studied by bio-layer interferometry (BLI). The C-region variants were coupled to the sensor tip, and the physiological partners served as analytes. Remarkably, all tested

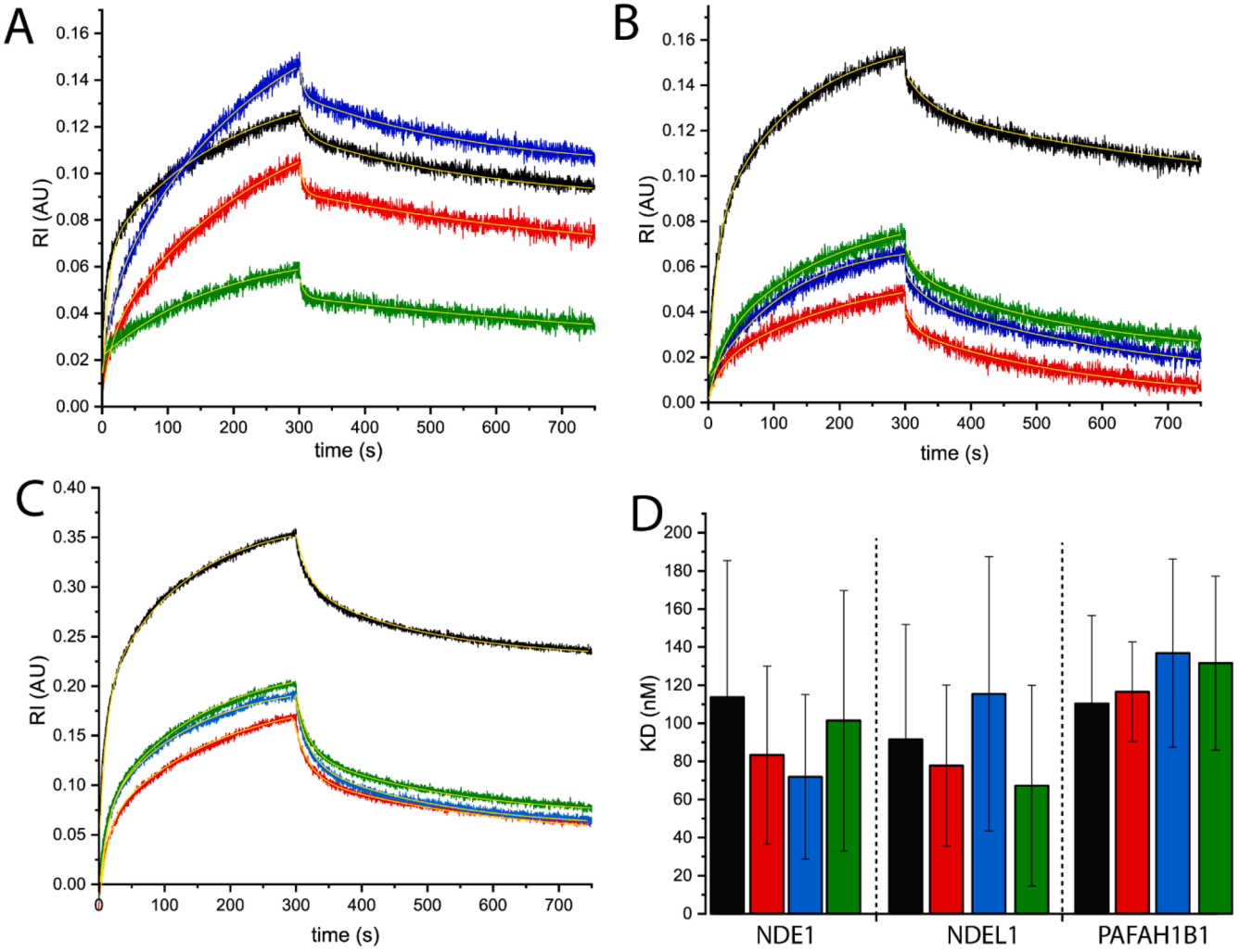


**Fig. 1.** BLI sensorgrams of (A) NDE1 (B) NDEL1, (C) PAFAH1B1 and (D) the binding affinity summary in bar plot (mean ± standard deviation) with WT C-region (black), S704C (red), S713E (blue) and L807-FS (green). The yellow solid line represents the exponential fittings to the kinetic data. The detailed analysis is provided in Tables 1 and **S1**.

C-region proteins interacted with the three proteins, NDE1, NDEL1 and PAFAH1B1. The kinetics of association and dissociation of the physiological partners to/from the C-region variants were similar (Fig. 1, Tables 1 and **S1**) under our experimental conditions, although the signal amplitudes differed markedly. Our findings thus provide a first indication that the clinically identified mutants bind to the physiological partners with similar sub-μM affinities as the WT C-region. This observation implies that the active sites for the interactions with the physiological partners in the mitotic spindle complex are not affected by and possibly located remote from the mutation sites. Thus, we hypothesize that the lynchpin motif facilitating the interaction is likely the β-core (717–761) that carries a pseudo-repeat sequence (Cukkemane et al., 2021). Additionally, it was not always possible to fit mono-exponential association/dissociation functions and hence we had to calculate the binding affinity using an average rate function (see Methodology). This suggests some heterogeneity within and between samples. This potential heterogeneity may have affected the immobilization efficiencies of the ligands. Thus, we resorted to CD spectropolarimetry to assess the state of the proteins in solution.

### 3.2. Stability of the C-region mutants

Freshly prepared samples were centrifuged to remove any large scattering particles prior to the CD experiments. Nevertheless, the presence of such aggregates was indirectly reflected in the CD spectra as a reduction in the signal intensities for the mutant variant samples (Fig. 2**A**). The L807-FS mutant showed a very weak ellipticity reading when compared with the ellipticity observed for the other C-region variants. This is in agreement with a previous report (Yerabham et al., 2017) where a decrease in the helical content of the frame shift mutant was observed over a period of 5 days. The S704C and the S713E mutant samples were relatively stable and yielded signals that were half the intensity of the WT C-region. Our attempts to deconvolute the spectra were not successful because the signal intensity in the far UV region in the 190–200 nm was very noisy. However, a qualitative evaluation of the spectra of the WT, S704C and S713E suggests the presence of helical and coiled elements. Taking into account of the normalized amplitudes of the different constructs in the CD spectra (Fig. 2**A**) indicates poor stability of the mutants in comparison to the WT-C-region that rapidly aggregate and thereby reduce the soluble protein concentration. Translating these observations to the full-length DISC1 protein, we speculate that reduced stability of the mutants may be the primary cause of DISC1-associated pathogenesis, with the mutations exacerbating aggregation.

### 3.3. The β-core is the minimal functional element that associates with physiological partners of the mitotic spindle complex

To address the second aspect of the hypothesis, i.e., whether the β-core is the functional lynchpin of the C-region, we performed BLI (Fig 2**B and 2 C**) and CD (Fig. 2**A**) measurements. Initially, the β-core was titrated against PAFAH1B1, NDEL1 or NDE1. As shown above for the WT C-region and its mutants, high-affinity binding in the sub-μM range to these physiological partners was observed. This finding strongly suggests that the pseudo-repeat sequence is an important functional entity, which corroborates cell biology experiments where the DISC1$^{\Delta 22aa}$ isoform lacks cell proliferative capability because of weak association with NDEL1 (Kamiya et al., 2006). Circular dichroism experiment on the normalized intensity of β-core (Fig. 2**A**) suggested that this region of DISC1 is highly unstable under in-vitro conditions and aggregates rapidly. Also, the spectra of β-core shows the presence of structured elements predominantly coiled but also presence of some helical content. However, CD measurements reported previously (Yerabham et al., 2017) indicated the β-core is exclusively unstructured. In the same report, the size-exclusion profile on two different samples of β-core resulted in profiles containing exclusively monomers and another populated with oligomers. Taken together, the results illustrate that the β-core is prone to oligomerization/aggregation and adopts several conformations, some of which are relevant for the function of the C-region. In this study, as we had centrifuged the sample prior to measurements, it is likely that we have removed the large aggregating disordered β-core and have a small population in solution.

Overall, these findings indicate that the mutations do not lead to inactive proteins when the β-core is preserved for association with physiological partners. Rather, the pathophysiology associated with the mutants arises because of their poor stability in solution.

**Table 1**
Binding affinities ($K_D$) of the physiological partners viz. NDEL1, NDE1 and PAFAH1B1 w.r.t. the different C-region variants and the β-core.

| | WT (nM) | S713E (nM) | S704C (nM) | L807-FS (nM) | β-core (nM) |
|---|---|---|---|---|---|
| PAFAH1B1 | 110.35 ± 46.18 | 136.86 ± 49.43 | 116.56 ± 26.19 | 131.60 ± 45.57 | 132.06 ± 38.07 |
| NDEL1 | 91.53 ± 60.34 | 115.43 ± 71.98 | 77.81 ± 42.23 | 67.19 ± 52.73 | 77.63 ± 42.61 |
| NDE1 | 113.71 ± 71.72 | 71.92 ± 43.17 | 83.35 ± 46.73 | 101.39 ± 68.39 | 105.04 ± 16.26 |

**Table 2**
Binding affinities ($K_D$) of the peptide therapeutics w.r.t. the different C-region variants.

| | Flo1 (nM) | Flm1 (nM) |
|---|---|---|
| WT | 97.6 | 146.3 |
| S704C | 156.0 | 78.0 |
| S713E | 73.4 | 81.0 |
| L807FS | 37.2 | 17.9 |

### 3.4. Structural model of the tetrameric DISC1 C-region

We performed chemical crosslinking-coupled MS of proteolytic fragments to identify sites of self-association and hence characterize the architecture of the C-region tetramer. However, in this case, we encountered serious challenges in identifying proteolytic fragments. We surmised that this problem was caused by the poor stability of the C-region proteins under in-vitro conditions, which may further be compounded by chemical modification during crosslinking. We then tested the WT C-region, the various C-region mutants, and the β-core in the presence of DSSO to identify potential interfacial regions. Under experimental conditions using DSSO as the cross-linker, we observed intra-subunit loop-links among the Lys residues, i.e., K741-K743, K743–K747, K747–K753, K753–K768, K787–K788 and K819–K833 (**Table S3**). Serendipitously, in a unique instance, we observed an inter-subunit crosslink (K741–K741) in the S704C sample (**Fig. S3**).

Starting from the AlphaFold2 model of the hDISC1 C-region protomer, we next generated tetramer models using ClusPro (Kozakov et al., 2017). We analyzed candidate structures for the plausibility of the K741-K741 crosslink within a distance of 10.1 Å, which represents the length of the chemical linker. Furthermore, we considered the longest axis of the model as a rough estimate relating to the $R_H$ of ~5 nm observed from DLS experiments. Only one model fulfilled the criteria (Fig. 3), whereas two models had acceptable solutions (**Fig. S4**) but were missing the inter-subunit cross-link possibility. Careful inspection of the model that fulfilled the restraints revealed that the β-core is an essential element for oligomerization, which is mediated by a short α-helix (745–755). Moreover, the disordered region in the β-core is exposed to solvent, thereby potentially offering conformational flexibility to associate with physiological partners. Lastly, in addition to K741-K741 that was obtained as an unambiguous inter-subunit restraint, the model suggests that inter- and intra-subunit cross-links for K741–K743 should

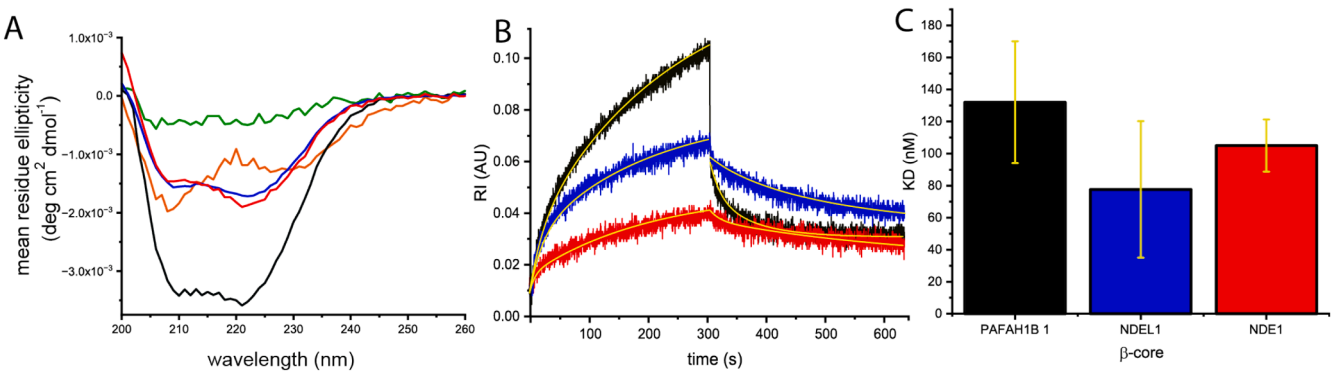


**Fig. 2.** (A) CD measurements of the various C-region constructs. β-core (orange), WT C-region (black), S713E (blue), S704C (red), and L807-FS (green). (B) BLI sensorgrams of the β-core binding to PAFAH1B1 (black) NDEL1 (blue) and NDE1 (red) with the fitted data shown in yellow. Results of the analysis are given in Tables 1 and **S1** and as a bar plot mean ± standard deviation in (C).

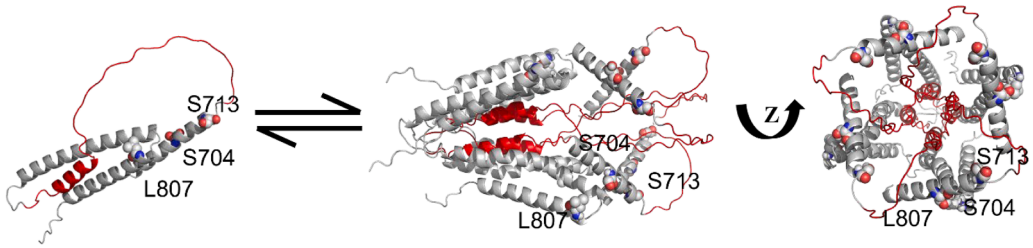


**Fig. 3.** Structural model of the DISC1 C-region. Left, model of the monomeric protein, as generated by AlphaFold2. Middle and right, tetrameric structure obtained by CLUSPRO docking. Based on the intra- and inter-subunit (**Table S2**) restraints that were derived from the MS-crosslinking experiments, the best-fitting model was selected. The residues that are affected by the mutations studied in this manuscript are shown in cpk (for Corey–Pauling–Koltun) mode, the β-core is drawn in red.

also be possible because these two residues are well within 10 Å.

### 3.5. Discovery of potential therapeutic peptides that target the C-region of DISC1

Phage display selection targeting the C-region of the protein was used as a strategy for developing drugs against DISC1 aggregation (Jaroszewicz et al., 2022). In this strategy (**Fig. S2**), we used a library containing phages that were decorated with 16-mer peptides. We identified several binding partners for the oligomeric and monomeric preparations of the WT DISC1 C-region. Next generation sequencing (NGS) was performed to identify the peptide hits, followed by several rounds of sequence filtering using TSAT (Santur et al., 2021) and HAMMOCK (Krejci et al., 2016). Finally, the empty and enrichment scores (**Fig. S5**) were calculated for the filtered sequences, and the peptides were ranked and selected on the basis of their empty and enrichment scores and the size of the generated clusters. From the several hits identified, we selected the highest-ranking peptide for both the monomeric and the oligomeric target (termed Flm01 and Flo01, respectively) for biophysical and structural characterization of the protein-peptide interaction.

### 3.6. Protein-peptide interactions

Flo01 and Flm01 were tested for their specific interactions with the DISC1 C-region. As a first step, the WT C-region of DISC1 was studied using BLI (Fig. 4**A and 4 B**), where the identified 16-mer peptides were immobilized to the sensor chip and the C-region served as the analyte. This approach was extended to study the interaction of the potential peptide therapeutics with the three clinically identified mutants. The peptides bound to the WT C-region and the mutant variants with affinities in the nM range (Fig. 4**C**) (Cukkemane and Willbold, 2022). Although the affinities were high, the kinetics for the interactions differed remarkably (**Table S3**). The basis of these differences was examined by solution NMR to probe the binding modes of the peptides, while the effects on DISC1 C-region aggregation were assessed by DLS.

### 3.7. DISC1 C-region aggregation is attenuated in the presence of potential peptide therapeutics

The selected peptides were further tested for their specific interactions with the WT DISC1 C-region. We tested the WT DISC1 C-region, which aggregated rapidly (< 30 min following centrifugation to remove visible aggregates). When challenged with equimolar concentrations of Flo01 (Fig. 4**D, 4 E and Fig. S6**) and Flm01 (Fig. 4**D**) the fibrillar growth kinetics were reduce markedly. During the experimental time window, the aggregates of the untreated C-region are larger than 250 nm in radius, whereas in the peptide-treated samples, the largest observable species had an apparent $R_H$ of ~50 nm. We also observed the presence of the tetramer when the protein:peptide ratio was maintained at 1:1 (Fig. 4**D**) for Flm01. This indicates that a higher concentration ratio of protein-ligand is required for inhibiting and/or curtailing aggregation. In a similar experimental setup, increasing concentrations of Flm01 yielded no further change in the kinetics of the aggregates. However, Flo01 at protein:peptide ratios of 1:5, 1:10 and 1:25 caused a clear decrease in the aggregate size, and at higher ratios a stable population of the tetramer was observed (Fig. 4**E**) over the duration of the DLS experiment. Additionally, a stable population with a $R_H$ of 12–16 nm was observed and we postulate that this population likely represents the oligomeric fraction of the C-region. This is because Flo01 was identified using the oligomeric species as the capture ligand. These promising results raise two interesting questions: how do the two peptides that were generated against two different species of the DISC1 C-region interact with the protein and which residues are critical for binding of the peptide drug?

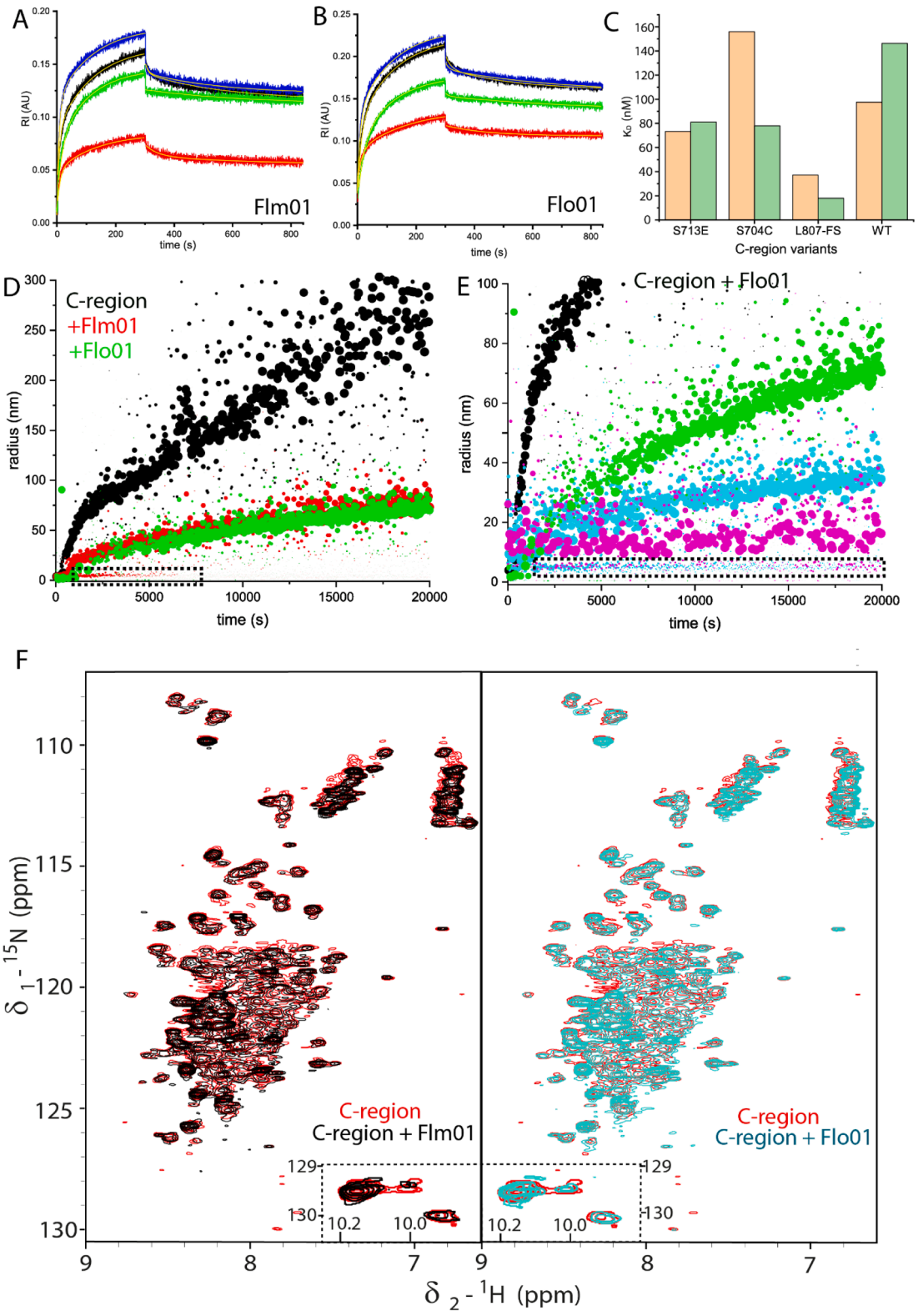


**Fig. 4.** BLI sensorgrams featuring binding of (A) Flm01 and (B) Flo01 to WT C-region (blue), S704C (red), S713E (black) and L807-FS (green). (C) The binding affinity of the peptides Flo01 (light brown) and Flm01 (green) to the various region constructs is shown in the bar plot, the details of which are provided in Tables 2 and **S3**. (D) Intensity-weighted DLS isotherms of the WT DISC1 C-region (10 μM, black) and equimolar mixtures with 16mer peptides Flm01 (red) and Flo01 (green). The dotted box represents the population of the tetrameric species. (E) Close-up (also refer to **Fig. S6** for the full isotherm) of a titration of the WT C-region (10 μM, black) with Flo01 at concentrations of 50 μM (green), 100 μM (cyan) and 250 μM (magenta). Again, the tetrameric population is marked by a dotted box. (F) Overlay of the 2D $^{1}$H–$^{15}$N HSQC spectra of unliganded C-region (75 μM, red) and the C-region bound to Flm01 (125 μM, black; left panel) and Flo01 (125 μM, cyan; right panel). Insets (dotted boxes) provide close-up views of the signals arising from the Trp indole side chains.

### 3.8. DISC1 C-region is intrinsically disordered in the absence of a physiological binding partner

Solution NMR was used to examine the conformation of the DISC1 C-region. The 2D $^{1}H–^{15}N$ heteronuclear single quantum coherence (HSQC) spectrum of the WT C-region showed low $^{1}H$ chemical shift (CS) dispersion of the peaks (Fig. 4**F**). Similar findings were reported previously (Cukkemane et al., 2021) and also for a truncated mDISC1 C-region (Ye et al., 2017). However, unlike the truncated mDISC1 C-region, where the spectral dispersion improved noticeably on binding a fragment from NDEL1 (Ye et al., 2017) or ATF4 (Wang et al., 2019) in the context of a fusion protein, the overall $^{1}H$ CS dispersion of the signals in the presence of either peptide (Fig. 4**F**) remained essentially unchanged, indicating no pronounced structural change occurred was formed on binding. Nonetheless, minor shifts were observed for a small subset of signals, indicating an interaction between peptide and protein. Increasing the peptide:protein ratio to values similar to those used in the DLS experiments also yielded small changes in the 2D $^{1}H$-$^{15}N$ HSQC spectrum (**Fig. S7**). The observed poor $^{1}H$ CS dispersion may reflect either intrinsic disorder or oligomerization or both. Considering the findings from the CD spectra (Fig. 2) and the DLS experiments ((Cukkemane et al., 2021), Fig. 4**D and 4 E**), we surmise that the DISC1 C-region can adopt various different conformations and exists as a tetramer and larger species and contains coiled-coil regions, as modeled by AlphaFold2 (Jumper et al., 2021) and reported previously (Wang et al., 2019; Ye et al., 2017), and intrinsically disordered regions (IDRs).

We investigated the CS changes upon binding of Flo01 and Flm01 to the WT C-region. CS perturbations of several distinguishable signals in the 2D $^{1}H–^{15}N$ HSQC spectra of the WT C-region in the presence of Flo01 were observed. Overall, the differences in the CS between the liganded and unliganded states are small. Even smaller CS changes are observed for signals from the WT C-region in the presence of Flm01. In both cases, residues within the IDRs may also interact with the peptides. However, the limited spectral dispersion precludes analysis of these interactions without resorting to various labeling strategies, solid-state NMR spectroscopy, or a combination of both, to obtain residue specific information of the binding interface of the protein-peptide complexes.

## 4. Discussion

In this report, we sought to understand the function of the DISC1 C-region by studying mutant variants. DISC1 function is associated with the initial stages of neurodevelopment, involving a regulatory role in the mitotic spindle complex (Bradshaw and Korth, 2019; Tropea et al., 2018; Yerabham et al., 2013), but its mechanism of action is still poorly understood. Do the mutations identified in patients actually render the C-region dysfunctional? To this extent, we performed BLI measurements on the different C-region mutant variants. The S704C mutant has previously been identified as aggregates in post-mortem brain tissue of patients suffering from schizophrenia, BD and MDD (Korth, 2012; Leliveld et al., 2009). Similarly, the L807-FS mutant was found to aggregate in subjects with debilitating mental illness (Sachs et al., 2005). In accordance with these data, we observed the S704C and the L807-FS variants to be severely aggregating, but to our surprise, aggregation was also obvious for the S713E protein. Interestingly, all tested mutants, displayed high-affinity binding in the sub-μM range with their physiological partners, NDEL1, NDE1 and PAFAH1B1. The WT C-region binds PAFAH1B1 (Cukkemane et al., 2021) and NDEL1 (Ye et al., 2017) with dissociation constants in the sub-μM range. Additionally, the S704C constitutes a silent mutation that is fully functional and capable of binding to NDEL1 (Kamiya et al., 2006; Leliveld et al., 2009; Narayanan et al., 2011). These findings strongly indicate that the mutations do not directly affect interaction with physiological binding partners, but that loss of function may secondarily arise because of protein aggregation. Studying these interactions is challenging because of protein instability (both ligands and analytes), which is reflected, by the large standard deviation of the binding constants. Lastly, we note one major difference with respect to our previous findings: We previously observed a μM binding affinity for the C-region and NDEL1 (Cukkemane et al., 2021), in contrast to the nM affinity reported here, which is consistent with the findings of Ye et al. (Ye et al., 2017). We believe the source of discrepancy may be the difficulty in handling the proteins as they are highly unstable in solution.

In the context of protein instability, the L807-FS mutant is a peculiar case among DISC1 mutants, because the region downstream of L807 was postulated to harbor a site critical for binding to NDEL1 (Brandon et al., 2004). The DISC1 segments interacting with NDEL1 have been a matter of intense debate, and regions other than the C-region have been shown to be involved (Kamiya et al., 2006; Morris et al., 2003). One of the strongest indicators that the NDEL1 binding site exists within the C-region is related to the DISC1$^{\Delta 22aa}$ splice variant, which binds only weakly to NDEL1. The 3D solution structure (Ye et al., 2017) of the truncated mDISC1-NDEL1 fusion protein is strongly supportive of this notion and highlights an amino acid stretch upstream of L807 that is also critical for the interaction with NDEL1. Herein, we showed that the β-core encompassing residues 716–761, which houses a major portion of the Δ22 region (748–769), is sufficient to bind to NDEL1, NDE1 and PAFAH1B1 with high affinity. In a previous report (Cukkemane et al., 2021), the β-core was shown to harbor a pseudo-repeat sequence, which is an important feature in amyloidogenic proteins. Indeed, a fibrillar WT C-region with the β-core serving as the fibrillar scaffold that is unavailable for other protein-protein interactions, would resemble the DISC1$^{\Delta 22aa}$ splice variant in its inability to bind physiological partners.

To better comprehend how the C-region, particularly the β-core, on one hand is able to bind physiological partners and on the other is susceptible to pathological effects, we derived a structural model. We first generated a template protomer of the C-region using AlphaFold2 (Jumper et al., 2021). The model of the monomer suggests that the β-core is sandwiched between a helix containing S704 and S713 and the coiled-coil domain that was observed experimentally using solution NMR spectroscopy (Wang et al., 2019; Ye et al., 2017). The β-core in the monomeric C-region is likely to display structural plasticity and dynamics to facilitate binding to various physiological partners. In the tetrameric state, the disordered region of the β-core is predicted to be exposed to solvent, enabling multivalent interaction. In analogy to fibril assembly pathways (Willbold et al., 2021) established for amyloidogenic proteins, where IDRs of a monomeric feeder protein transform into the cross-β scaffold of fibrils, we hypothesize monomeric DISC1 to serve as the building block for fibrillization.

Based on our findings, previously reported data (Cukkemane et al., 2021) and the recent success of phase-I clinical trials of the therapeutic d-enantiomeric peptide RD2 (Schemmert et al., 2019) in eliminating Aβ oligomers for treating Alzheimer's disease piqued our interest in identifying peptide drugs targeting DISC1 using a similar approach. We initiated a selection using monomeric and oligomeric C-region proteins as bait to identify peptide binders. Two lead peptides, one identified against the monomer (Flm1) and the other against the oligomer (Flo1), displayed nanomolar affinities (Fig 4**A and 4 B**; (Cukkemane and Willbold, 2022)) to the DISC1 WT C-region and mutants. Although both peptides did not abolish aggregation of the WT C-region, they remarkably slowed the kinetics of fibril growth and successfully curtailed the formation of large particles (see Fig. 5 for proposed model). At a protein-to-peptide ratio of 1:1, both peptides reduced C-region aggregate sizes throughout the experiment (Fig. 4**D**). Remarkably, when applied at tenfold excess, Flo1 (Fig 4**E**) was even able to bring particle sizes down to 12 to 16 nm, possibly representing the oligomeric species that was used for its selection. These findings open a whole new avenue and a wide range of applications. On the one hand, the peptides can be used to capture DISC1 from blood and/or CSF as a diagnostic marker. On the other hand, they might be further modified and improved for application as therapeutic agents, with the aim to limit or prevent formation of DISC1 aggregates and/or fibrils.

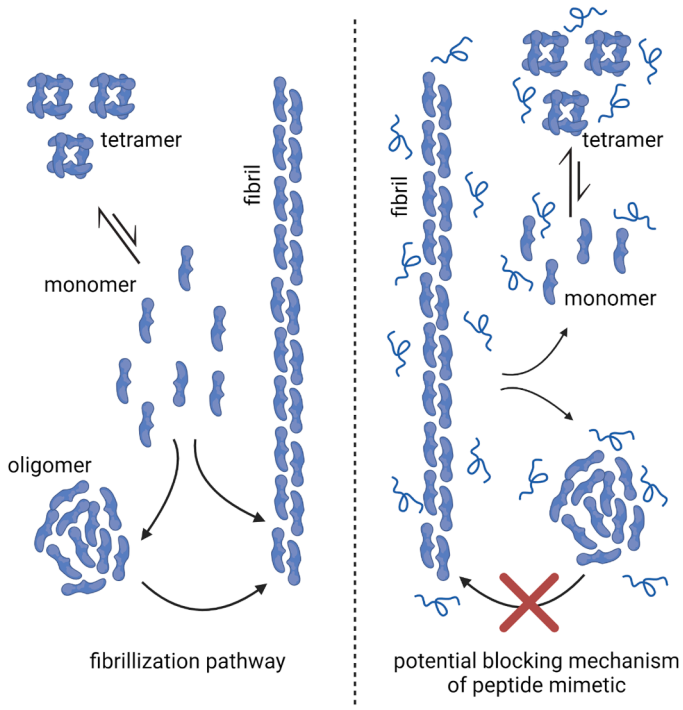


**Fig. 5.** Schematic illustration of the potential activity of the peptide mimetic. In the absence of the peptide (left panel) the monomer is in equilibrium with the tetramer under physiological conditions. Under atypical conditions, the monomer serves the role of the building block for the formation of oligomers and fibrils. In the presence of the peptide (right panel), we postulate that the peptide interacts with the monomers in a competitive manner such that a competition ensues for the monomer between the peptide and the aggregates. This results in curtailing the kinetics and the size of the aggregates. In the case of Flo01, at sufficiently high concentrations, the oligomeric species is stabilized along with the tetramer that can no longer participate in the formation of fibrils, while in Flm01 the reaction continues to proceed albeit with slow growth kinetics.

Impressed by the activity of the peptides, we next proceeded to characterize residue-specific interactions between the WT C-region and the peptide ligands using solution NMR spectroscopy. The finding of only minor chemical shift changes for a limited number of C-region resonances is intriguing given that the peptides bind to the protein with high affinity and significantly affect its self-association kinetics. Notably, similar minor peak shifts in NMR data have been reported for the ultrahigh affinity complex between the two intrinsically disordered proteins histone H1 and ProTα (Borgia et al., 2018). In this study, complex formation involves a large number of opposite charge interactions without defined interacting residues or sites. We hypothesize that a similar situation exists for the interaction between DISC1 and the 16mer peptides, with long-range electrostatic attraction mediating the high affinity interaction between the two polypeptide chains. Although the affinity between the peptide and the C-region involves high-affinity binding in the nm range, we require higher ratios of the peptide to slow the kinetics of aggregation growth to near stabilization of the population of the oligomers and tetramers (Figs 4**D** and **4 E**). However, the formation of aggregates and fibrils is also highly favored thermodynamically, with a binding affinity of the C-region monomers to the fibrils of ~750 nm (Cukkemane et al., 2021). This results in a competition between the peptides and the aggregates for the free monomers in the solution (Fig 5). Based on the results from the DLS, we observe a slow tonic increase in the size of the aggregates (Figs 4**D**) at a stoichiometry of 1:1. However at higher, concentrations of the peptide namely, Flo01, we see a total inhibition of the formation of the aggregates and stabilization of the potentially oligomeric fraction and the tetrameric species.

Despite these promising results, admittedly several limitations persist. First, both the C-region protein and its variants exhibited significant instability due to poor solubility, particularly in the case of the L807-FS mutant. This compromised protein handling and likely contributed to the observed variability in binding affinity measurements. More importantly, extrapolating these findings to the full-length DISC1 protein presents an even greater challenge, because the protein contains several intrinsically disordered and aggregation-prone regions that complicate biochemical analysis. Second, the following study is purely biophysical in nature. It limits our ability to infer therapeutic potential of the peptide mimetics from the application point-of-view to assess the biological efficacy, toxicity, or pharmacodynamics of the peptides. Third, the pharmacokinetics and metabolic stability of the peptides have not yet been evaluated. As L-enantiomeric drugs are susceptible to proteolytic degradation, it is necessary to conduct in-vitro and in-vivo tests on the d-enantiomeric versions for therapeutic use as drug candidates. These limitations highlight the need for further validation in cellular and animal models.

## 5. Conclusion

In summary, folding and aggregation of proteins are two sides of the same coin (Pastore and Temussi, 2012). Proteinopathic agents more often contain large stretches of IDRs (Lapidus, 2013). In the absence of a physiological partner, the unstructured regions likely exist in a dynamic equilibrium. Together with the coiled-coil domain, the IDR structures provide ample freedom for DISC1 to associate with a plethora of potential partners, and we were able to narrow down the segment that binds components of the mitotic spindle complex (NDEL1, NDE1, PAFAH1B1) to the β-core (716-761). We also showed that disease-associated mutations in the C-region do not directly affect protein function, but rather influence protein stability.

Lastly, we describe a potential target for treating psychotic disorders with a strategy that does not involve prospective drugs of low molecular weight (< 900 Da). Most forms of therapy that exist today are empirical. They comprise the 2nd and 3rd generation atypical antipsychotics (Paul and Potter, 2023), which target dopamine receptors (D2R) and, recently, also serotonin receptors (5HTR), and primarily serve to treat symptoms (mostly psychotic) and preserve remaining abilities. Therefore, it is essential to identify molecular structures that are critical for pathogenesis and target them for causal intervention. Using the phage-display strategy, we demonstrate the selection of lead peptides directed at monomeric and oligomeric states of the C-region that are capable of slowing down the fibrillization kinetics. This raises further potential to develop new strategies for drug development targeting risk factors for schizophrenia, bipolar disorder, major depressive disorder, and related chronic mental illnesses.

In order to realize the full potential of the peptide mimetics as therapeutic candidates, it is essential to address the limitations mentioned above that requires several critical steps. This includes optimizing peptide stability through chemical modifications such as cyclization, incorporation of non-natural amino acids, or PEGylation, which may significantly enhance their resistance to degradation, improve their pharmacokinetic properties and bioavailability. Among these one of the most successfully implemented methodologies in our group has been the use of d-enantiomeric peptides (Funke and Willbold, 2012), which were generated using mirror-image phage display technique (Sun et al., 2012). Notably, this method has already yielded the therapeutic peptide PRI-002, which has successfully completed Phase Ib (Kutzsche et al., 2025) is currently undergoing Phase II clinical trials for Alzheimer's disease. As the quintessential next step, we plan to evaluate the efficacy and safety of the peptides in DISC1 mouse models namely Tg (tetO-DISC1*)1001Plet (Pletnikov et al., 2008) and the DISC1-Boymaw (Zhou et al., 2010). In the near future, we aim to complete the pre-clinical trials to assess the peptides' mechanism of action in mice models, identify potential off-target effects, and explore formulations

that support clinical delivery. All these efforts together will be crucial for translating these biophysically validated peptide leads into clinically viable candidates for CMIs.

## CRediT authorship contribution statement

**Abhishek Cukkemane:** Writing – review & editing, Writing – original draft, Validation, Supervision, Project administration, Methodology, Investigation, Data curation, Conceptualization. **Andrew J. Dingley:** Writing – review & editing, Validation, Methodology, Investigation. **Jeannine Mohrlüder:** Writing – review & editing, Methodology, Investigation. **Beatrix Santiago-Schübel:** Writing – review & editing, Methodology, Investigation. **Oliver H. Weiergräber:** Writing – review & editing, Writing – original draft, Resources, Project administration, Formal analysis, Conceptualization. **Dieter Willbold:** Writing – review & editing, Writing – original draft, Validation, Supervision, Resources, Project administration, Investigation, Funding acquisition, Conceptualization.

## Declaration of competing interest

A.C. and D.W. are co-inventor of patents covering the peptide drugs. All other authors declare no competing interests.

## Acknowledgments

We thank the Biologisch Medizinisches Forschungszentrum of the Heinrich Heine University Düsseldorf for performing the NGS analysis. Access to the Jülich-Düsseldorf Biomolecular NMR Center jointly run by Forschungszentrum Jülich and HHU, and supported by the DFG (HE 3243/4–1 and INST 208/771–1 FUGG) are acknowledged. We also thank the Alexander von Humboldt foundation (Ref 3.4 – 1142747 – HRV – IP) for financial support.

## Supplementary materials

Supplementary material associated with this article can be found, in the online version, at doi:10.1016/j.ejps.2025.107148.

## Data availability

No data was used for the research described in the article.

## References

Altendorf, T., Mohrluder, J., Willbold, D., 2024. TSAT: efficient evaluation software for NGS data of phage/mirror-image phage display selections. Biophys Rep (N Y) 4 (3), 100166. https://doi.org/10.1016/j.bpr.2024.100166.

Beck, S., Michalski, A., Raether, O., Lubeck, M., Kaspar, S., Goedecke, N., Baessmann, C., Hornburg, D., Meier, F., Paron, I., Kulak, N.A., Cox, J., Mann, M., 2015. The Impact II, a very high-resolution quadrupole time-of-flight instrument (QTOF) for deep shotgun proteomics. Mol Cell Proteomics 14 (7), 2014–2029. https://doi.org/10.1074/mcp.M114.047407.

Blackwood, D.H.R., Fordyce, A., Walker, M.T., St Clair, D.M., Porteous, D.J., Muir, W.J., 2001. Schizophrenia and affective disorders - cosegregation with a translocation at chromosome 1q42 that directly disrupts brain-expressed genes: clinical and P300 findings in a family. Am. J. Hum. Genet. 69 (2), 428–433. https://doi.org/10.1086/321969.

Borgia, A., Borgia, M.B., Bugge, K., Kissling, V.M., Heidarsson, P.O., Fernandes, C.B., Sottini, A., Soranno, A., Buholzer, K.J., Nettels, D., Kragelund, B.B., Best, R.B., Schuler, B., 2018. Extreme disorder in an ultrahigh-affinity protein complex. Nature 555 (7694), 61–66. https://doi.org/10.1038/nature25762.

Bradshaw, N.J., Korth, C., 2019. Protein misassembly and aggregation as potential convergence points for non-genetic causes of chronic mental illness. Mol Psychiatry 24 (7), 936–951. https://doi.org/10.1038/s41380-018-0133-2.

Brandon, N.J., Handford, E.J., Schurov, I., Rain, J.C., Pelling, M., Duran-Jimeniz, B., Camargo, L.M., Oliver, K.R., Beher, D., Shearman, M.S., Whiting, P.J., 2004. Disrupted in Schizophrenia 1 and Nudel form a neurodevelopmentally regulated protein complex: implications for schizophrenia and other major neurological disorders. Mol Cell Neurosci 25 (1), 42–55. https://doi.org/10.1016/j.mcn.2003.09.009.

Cukkemane, A., Becker, N., Zielinski, M., Frieg, B., Lakomek, N.A., Heise, H., Schroder, G.F., Willbold, D., Weiergraber, O.H., 2021. Conformational heterogeneity coupled with beta-fibril formation of a scaffold protein involved in chronic mental illnesses. Transl Psychiatry 11 (1), 639. https://doi.org/10.1038/s41398-021-01765-1.

Cukkemane, A., & Willbold, D. (2022). DISC1-binding peptides and the use thereof for the treatment and diagnosis of schizophrenia, major depressive disorders (MDD), and bipolar disorders (BD), and autism and other chronic mental disorders (CMDS). (PCT/EP2023/066796).

Funke, S.A., Willbold, D., 2012. Peptides for therapy and diagnosis of Alzheimer's disease. Curr Pharm Des 18 (6), 755–767. https://doi.org/10.2174/138161212799277752.

Hashimoto, R., Numakawa, T., Ohnishi, T., Kumamaru, E., Yagasaki, Y., Ishimoto, T., Mori, T., Nemoto, K., Adachi, N., Izumi, A., Chiba, S., Noguchi, H., Suzuki, T., Iwata, N., Ozaki, N., Taguchi, T., Kamiya, A., Kosuga, A., Tatsumi, M., Kunugi, H., 2006. Impact of the DISC1 Ser704Cys polymorphism on risk for major depression, brain morphology and ERK signaling. Hum. Mol. Genet. 15 (20), 3024–3033. https://doi.org/10.1093/hmg/ddl244.

Hikida, T., Gamo, N.J., Sawa, A., 2012. DISC1 as a therapeutic target for mental illnesses. Expert Opin. Ther. Targets 16 (12), 1151–1160. https://doi.org/10.1517/14728222.2012.719879.

Hughes, C.S., Moggridge, S., Muller, T., Sorensen, P.H., Morin, G.B., Krijgsveld, J., 2019. Single-pot, solid-phase-enhanced sample preparation for proteomics experiments. Nat Protoc 14 (1), 68–85. https://doi.org/10.1038/s41596-018-0082-x.

Ishizuka, K., Kamiya, A., Oh, E.C., Kanki, H., Seshadri, S., Robinson, J.F., Murdoch, H., Dunlop, A.J., Kubo, K., Furukori, K., Huang, B., Zeledon, M., Hayashi-Takagi, A., Okano, H., Nakajima, K., Houslay, M.D., Katsanis, N., Sawa, A., 2011. DISC1-dependent switch from progenitor proliferation to migration in the developing cortex. Nature 473 (7345), 92–96. https://doi.org/10.1038/nature09859.

Jaroszewicz, W., Morcinek-Orlowska, J., Pierzynowska, K., Gaffke, L., Wegrzyn, G., 2022. Phage display and other peptide display technologies. FEMS Microbiol Rev 46 (2). https://doi.org/10.1093/femsre/fuab052.

Jumper, J., Evans, R., Pritzel, A., Green, T., Figurnov, M., Ronneberger, O., Tunyasuvunakool, K., Bates, R., Zidek, A., Potapenko, A., Bridgland, A., Meyer, C., Kohl, S.A.A., Ballard, A.J., Cowie, A., Romera-Paredes, B., Nikolov, S., Jain, R., Adler, J., Hassabis, D., 2021. Highly accurate protein structure prediction with AlphaFold. Nature 596 (7873), 583–589. https://doi.org/10.1038/s41586-021-03819-2.

Kamiya, A., Tan, P.L., Kubo, K., Engelhard, C., Ishizuka, K., Kubo, A., Tsukita, S., Pulver, A.E., Nakajima, K., Cascella, N.G., Katsanis, N., Sawa, A., 2008. Recruitment of PCM1 to the centrosome by the cooperative action of DISC1 and BBS4: a candidate for psychiatric illnesses. Arch Gen Psychiatry 65 (9), 996–1006. https://doi.org/10.1001/archpsyc.65.9.996.

Kamiya, A., Tomoda, T., Chang, J., Takaki, M., Zhan, C., Morita, M., Cascio, M.B., Elashvili, S., Koizumi, H., Takanezawa, Y., Dickerson, F., Yolken, R., Arai, H., Sawa, A., 2006. DISC1-NDEL1/NUDEL protein interaction, an essential component for neurite outgrowth, is modulated by genetic variations of DISC1. Hum. Mol. Genet. 15 (22), 3313–3323. https://doi.org/10.1093/hmg/ddl407.

Korth, C., 2012. Aggregated proteins in schizophrenia and other chronic mental diseases: DISC1opathies. Prion 6 (2), 134–141. https://doi.org/10.4161/pri.18989.

Kozakov, D., Hall, D.R., Xia, B., Porter, K.A., Padhorny, D., Yueh, C., Beglov, D., Vajda, S., 2017. The ClusPro web server for protein-protein docking. Nat Protoc 12 (2), 255–278. https://doi.org/10.1038/nprot.2016.169.

Krejci, A., Hupp, T.R., Lexa, M., Vojtesek, B., Muller, P., 2016. Hammock: a hidden Markov model-based peptide clustering algorithm to identify protein-interaction consensus motifs in large datasets. Bioinformatics 32 (1), 9–16. https://doi.org/10.1093/bioinformatics/btv522.

Kutzsche, J., Cosma, N.C., Kauselmann, G., Fenski, F., Bieniek, C., Bujnicki, T., Pils, M., Bannach, O., Willbold, D., Peters, O., 2025. Oral PRI-002 treatment in patients with MCI or mild AD: a randomized, double-blind phase 1b trial. Nat Commun 16 (1), 4180. https://doi.org/10.1038/s41467-025-59295-z.

Lapidus, L.J., 2013. Understanding protein aggregation from the view of monomer dynamics. Mol Biosyst 9 (1), 29–35. https://doi.org/10.1039/c2mb25334h.

Lee, W., Tonelli, M., Markley, J.L., 2015. NMRFAM-SPARKY: enhanced software for biomolecular NMR spectroscopy. Bioinformatics 31 (8), 1325–1327. https://doi.org/10.1093/bioinformatics/btu830.

Leliveld, S.R., Bader, V., Hendriks, P., Prikulis, I., Sajnani, G., Requena, J.R., Korth, C., 2008. Insolubility of disrupted-in-schizophrenia 1 disrupts oligomer-dependent interactions with nuclear distribution element 1 and is associated with sporadic mental disease. Journal of Neuroscience 28 (15), 3839–3845. https://doi.org/10.1523/JNEUROSCI.5389-07.2008.

Leliveld, S.R., Hendriks, P., Michel, M., Sajnani, G., Bader, V., Trossbach, S., Prikulis, I., Hartmann, R., Jonas, E., Willbold, D., Requena, J.R., Korth, C., 2009. Oligomer assembly of the C-terminal DISC1 domain (640-854) is controlled by self-association motifs and disease-associated polymorphism S704C. Biochemistry 48 (32), 7746–7755. https://doi.org/10.1021/bi900901e.

Millar, J.K., Christie, S., Porteous, D.J., 2003. Yeast two-hybrid screens implicate DISC1 in brain development and function. Biochem. Biophys. Res. Commun. 311 (4), 1019–1025. https://doi.org/10.1016/j.bbrc.2003.10.101.

Millar, J.K., Wilson-Annan, J.C., Anderson, S., Christie, S., Taylor, M.S., Semple, C.A.M., Devon, R.S., St Clair, D.M., Muir, W.J., Blackwood, D.H.R., Porteous, D.J., 2000. Disruption of two novel genes by a translocation co-segregating with schizophrenia. Hum. Mol. Genet. 9 (9), 1415–1423. https://doi.org/10.1093/hmg/9.9.1415.

Morris, J.A., Kandpal, G., Ma, L., Austin, C.P., 2003. DISC1 (Disrupted-In-Schizophrenia 1) is a centrosome-associated protein that interacts with MAP1A, MIPT3, ATF4/5

and NUDEL: regulation and loss of interaction with mutation. Hum. Mol. Genet. 12 (13), 1591–1608. https://doi.org/10.1093/hmg/ddg162.
Narayanan, S., Arthanari, H., Wolfe, M.S., Wagner, G., 2011. Molecular characterization of disrupted in schizophrenia-1 risk variant S704C reveals the formation of altered oligomeric assembly. J Biol Chem 286 (51), 44266–44276. https://doi.org/10.1074/jbc.M111.271593.
Pastore, A., Temussi, P.A., 2012. The two faces of Janus: functional interactions and protein aggregation. Curr Opin Struct Biol 22 (1), 30–37. https://doi.org/10.1016/j.sbi.2011.11.007.
Paul, S.M., Potter, W.Z., 2023. Finding new and better treatments for psychiatric disorders. Neuropsychopharmacology. https://doi.org/10.1038/s41386-023-01690-5.
Pletnikov, M.V., Ayhan, Y., Nikolskaia, O., Xu, Y., Ovanesov, M.V., Huang, H., Mori, S., Moran, T.H., Ross, C.A., 2008. Inducible expression of mutant human DISC1 in mice is associated with brain and behavioral abnormalities reminiscent of schizophrenia. Mol Psychiatry 13 (2), 173–186. https://doi.org/10.1038/sj.mp.4002079, 115.
Rappsilber, J., Ishihama, Y., Mann, M., 2003. Stop and go extraction tips for matrix-assisted laser desorption/ionization, nanoelectrospray, and LC/MS sample pretreatment in proteomics. Anal Chem 75 (3), 663–670. https://doi.org/10.1021/ac026117i.
Sachs, N.A., Sawa, A., Holmes, S.E., Ross, C.A., DeLisi, L.E., Margolis, R.L., 2005. A frameshift mutation in Disrupted in Schizophrenia 1 in an American family with schizophrenia and schizoaffective disorder. Mol Psychiatry 10 (8), 758–764. https://doi.org/10.1038/sj.mp.4001667.
Santur, K., Reinartz, E., Lien, Y., Tusche, M., Altendorf, T., Sevenich, M., Tamguney, G., Mohrluder, J., Willbold, D., 2021. Ligand-induced stabilization of the native Human superoxide dismutase 1. ACS Chem Neurosci 12 (13), 2520–2528. https://doi.org/10.1021/acschemneuro.1c00253.
Schemmert, S., Schartmann, E., Honold, D., Zafiu, C., Ziehm, T., Langen, K.J., Shah, N.J., Kutzsche, J., Willuweit, A., Willbold, D., 2019. Deceleration of the neurodegenerative phenotype in pyroglutamate-Abeta accumulating transgenic mice by oral treatment with the Abeta oligomer eliminating compound RD2. Neurobiol Dis 124, 36–45. https://doi.org/10.1016/j.nbd.2018.10.021.
Soares, D.C., Bradshaw, N.J., Zou, J., Kennaway, C.K., Hamilton, R.S., Chen, Z.A., Wear, M.A., Blackburn, E.A., Bramham, J., Bottcher, B., Millar, J.K., Barlow, P.N., Walkinshaw, M.D., Rappsilber, J., Porteous, D.J., 2012a. The mitosis and neurodevelopment proteins NDE1 and NDEL1 form dimers, tetramers, and polymers with a folded back structure in solution. J Biol Chem 287 (39), 32381–32393. https://doi.org/10.1074/jbc.M112.393439.
Soares, D.C., Bradshaw, N.J., Zou, J., Kennaway, C.K., Hamilton, R.S., Chen, Z.A., Wear, M.A., Blackburn, E.A., Bramham, J., Bottcher, B., Millar, J.K., Barlow, P.N., Walkinshaw, M.D., Rappsilber, J., Porteous, D.J., 2012b. The mitosis and neurodevelopment proteins NDE1 and NDEL1 form dimers, tetramers, and polymers with a folded back structure in solution. Journal of Biological Chemistry 287 (39), 32381–32393. https://doi.org/10.1074/jbc.M112.393439.
Sun, N., Funke, S.A., Willbold, D., 2012. Mirror image phage display–generating stable therapeutically and diagnostically active peptides with biotechnological means. J Biotechnol 161 (2), 121–125. https://doi.org/10.1016/j.jbiotec.2012.05.019.
Tanaka, M., Ishizuka, K., Nekooki-Machida, Y., Endo, R., Takashima, N., Sasaki, H., Komi, Y., Gathercole, A., Huston, E., Ishii, K., Hui, K.K., Kurosawa, M., Kim, S.H., Nukina, N., Takimoto, E., Houslay, M.D., Sawa, A., 2017. Aggregation of scaffolding protein DISC1 dysregulates phosphodiesterase 4 in Huntington's disease. J Clin Invest 127 (4), 1438–1450. https://doi.org/10.1172/JCI85594.
Taylor, M.S., Devon, R.S., Millar, J.K., Porteous, D.J., 2003. Evolutionary constraints on the disrupted in Schizophrenia locus. Genomics 81 (1), 67–77. https://doi.org/10.1016/s0888-7543(02)00026-5.
Tropea, D., Hardingham, N., Millar, K., Fox, K., 2018. Mechanisms underlying the role of DISC1 in synaptic plasticity. Journal of Physiology-London 596 (14), 2747–2771. https://doi.org/10.1113/Jp274330.
van Os, J., Kapur, S., 2009. Schizophrenia. Lancet 374 (9690), 635–645. https://doi.org/10.1016/S0140-6736(09)60995-8.
Wang, X., Ye, F., Wen, Z., Guo, Z., Yu, C., Huang, W.K., Rojas Ringeling, F., Su, Y., Zheng, W., Zhou, G., Christian, K.M., Song, H., Zhang, M., Ming, G.L., 2019. Structural interaction between DISC1 and ATF4 underlying transcriptional and synaptic dysregulation in an iPSC model of mental disorders. Mol Psychiatry. https://doi.org/10.1038/s41380-019-0485-2.
Willbold, D., Strodel, B., Schroder, G.F., Hoyer, W., Heise, H., 2021. Amyloid-type protein aggregation and prion-like properties of amyloids. Chem Rev 121 (13), 8285–8307. https://doi.org/10.1021/acs.chemrev.1c00196.
Wishart, D.S., Bigam, C.G., Yao, J., Abildgaard, F., Dyson, H.J., Oldfield, E., Markley, J. L., Sykes, B.D., 1995. 1H, 13C and 15N chemical shift referencing in biomolecular NMR. J. Biomol. NMR 6 (2), 135–140. https://doi.org/10.1007/BF00211777.
Ye, F., Kang, E., Yu, C., Qian, X., Jacob, F., Yu, C., Mao, M., Poon, R.Y.C., Kim, J., Song, H., Ming, G.L., Zhang, M., 2017. DISC1 Regulates neurogenesis via modulating kinetochore attachment of Ndel1/Nde1 during mitosis. Neuron 96 (5), 1204. https://doi.org/10.1016/j.neuron.2017.11.034.
Yerabham, A.S., Weiergraber, O.H., Bradshaw, N.J., Korth, C., 2013. Revisiting disrupted-in-schizophrenia 1 as a scaffold protein. Biol Chem 394 (11), 1425–1437. https://doi.org/10.1515/hsz-2013-0178.
Yerabham, A.S.K., Mas, P.J., Decker, C., Soares, D.C., Weiergraber, O.H., Nagel-Steger, L., Willbold, D., Hart, D.J., Bradshaw, N.J., Korth, C., 2017. A structural organization for the Disrupted in Schizophrenia 1 protein, identified by high-throughput screening, reveals distinctly folded regions, which are bisected by mental illness-related mutations. J Biol Chem 292 (16), 6468–6477. https://doi.org/10.1074/jbc.M116.773903.
Yerabham, A.S.K., Muller-Schiffmann, A., Ziehm, T., Stadler, A., Kober, S., Indurkhya, X., Marreiros, R., Trossbach, S.V., Bradshaw, N.J., Prikulis, I., Willbold, D., Weiergraber, O.H., Korth, C., 2018. Biophysical insights from a single chain camelid antibody directed against the disrupted-in-Schizophrenia 1 protein. PLoS One 13 (1), e0191162. https://doi.org/10.1371/journal.pone.0191162.
Yilmaz, S., Busch, F., Nagaraj, N., Cox, J., 2022. Accurate and automated high-coverage identification of chemically cross-linked peptides with MaxLynx. Anal Chem 94 (3), 1608–1617. https://doi.org/10.1021/acs.analchem.1c03688.
Yumerefendi, H., Tarendeau, F., Mas, P.J., Hart, D.J., 2010. ESPRIT: an automated, library-based method for mapping and soluble expression of protein domains from challenging targets. J Struct Biol 172 (1), 66–74. https://doi.org/10.1016/j.jsb.2010.02.021.
Zhou, X., Chen, Q., Schaukowitch, K., Kelsoe, J.R., Geyer, M.A., 2010. Insoluble DISC1-Boymaw fusion proteins generated by DISC1 translocation. Mol Psychiatry 15 (7), 669–672. https://doi.org/10.1038/mp.2009.127.